Automatic detection and repairing of cloud and shadow regions in multi-spectral remote sensing images

ZHOU Wei[1], GUAN Jian[1], JIANG Tao[2], HE You[1]

1. *Department of Electronic and Information Engineering, Naval Aeronautical and Astronautical University, Yantai* 264001, *China*;
2. *Department of Ordnance Science and Technology, Naval Aeronautical and Astronautical University, Yantai* 264001, *China*

Abstract: Clouds and their shadows in remote sensing images bring many troubles to image interpretation and application. It is important to detect and repair these regions rapidly. An efficient method was proposed to detect and repair the unwanted clouds and shadows using two images of the same site acquired in adjacent time. At first, the cloud and shadow regions were enhanced by fusing multi-spectral data and then detected automatically using Otsu's algorithm. Since the clouds and their shadows will lead to obvious differences in brightness between the two images, false detection of highlighted objects and water regions can be easily discarded, and then the normalized cloud and shadow density map can be built. Linear combination of two images and histogram matching algorithm were adopted to repair the shadow and cloud regions. Experiments on SPOT 4 multi-spectral remote sensing data show impressive results which will benefit several applications.

Key words: automatic detection, image repairing, histogram matching, cloud and shadow density map, multi-spectral

CLC number: TP751 **Document code:** A

Citation format: Zhou W, Guan J, Jiang T and He Y. 2012. Automatic detection and repairing of cloud and shadow regions in multi-spectral remote sensing images. Journal of Remote Sensing, 16(1): 132–142

1 INTRODUCTION

Due to weather such as cloud and fog, remote sensing images acquired by optical satellites may appear patches of bright cloud and dark shadow regions, which concealed ground objects partially or entirely. The inevitable information lose or interference may influence the correctness of target detection, recognition and classification, and bring great troubles in interpretation and application of remote sensing images (Wang, et al., 2004). Detection and repairing the regions influenced by cloud and shadow is the first problem (Song, et al., 2003; Song, et al., 2006; Chai, et al., 2010), to which many application researchers have to face.

Different schemes are needed to process different cloud and shadow types. Thin cloud may blur the image, but the objects are not concealed entirely. Zhao and Zhu (1996) proposed to remove thin cloud from great areas using homomorphic filter, which combines the frequency filtering and grayscale change to discriminate clouds and background, and remove the influence of cloud finally. Due to the limits of selected filter structure and cut-off frequency, some useful information may be discarded. Large patches of thick cloud concealed not only the objects in sight of sensor but also cast patches of shadow. An effective scheme is to replace the thick cloud regions with cloud free data acquired in adjacent time or same season in different years (Ri, et al., 2010). Because of the influence of object and imaging condition change, the repairing effect is determined by the similarity between the data to be repaired and cloud free data, and since precise registration and careful adjustment are necessary, more process time is needed.

In littoral area, even in fine weather, some cloud patch with different sizes and shapes may float in middle or low sky. Although the whole visual effect is well, the scattered cloud and their shadows may conceal part of ground object, which makes it difficult to interpret the image and produce intelligence media. We proposed an effective algorithm to detect and repair the cloud and shadow in multi-spectral images automatically. The algorithm needs two images acquired in adjacent time of the same area. At first, the cloud and shadow regions were enhanced by fusing multi-spectral data and then were detected automatically using Otsu's algorithm (Otsu, 1979). The obvious differences in brightness between the two images were used to discard the false detection of highlighted objects and water regions. Having constructed the normalized cloud and shadow density map, linear combination of two images and histogram matching algorithm were adopted to repair the shadow and cloud regions subsequently. We test

Received: 2010-10-22; **Accepted:** 2011-06-21

Foundation: National Natural Science Foundation of China (No. 60672140, 60802088); Aero-Science Foundation of China (No. 20095184004)

First author biography: ZHOU Wei (1980—), male, lecturer, Ph.D. candidate, he majors in reconnaissance image processing, target detection and recognition. E-mail: yeaweam@gmail.com

Corresponding author biography: GUAN Jian(1968—), male, professor, his research interests are radar target automatic detection, reconnaissance image processing, and information fusion. E-mail: guanjian96@tsinghua.org.cn

our algorithm on SPOT 4 multi-spectral remote sensing data and give the impressive results.

2 ANALYSIS THE CHARACTERISTIC OF CLOUD AND SHADOW

From the viewpoint of remote sensing physics, cloud belongs to atmospheric aerosol, which is a colloidal suspension of particles dispersed in air with certain stability, small sedimentation velocity, scaled in 0.001—10 μm. Considering the characteristics of reflection, in the visible bands, the cloud belongs to diffuse reflection object, which corresponds to regions of great local intensity, large regional mean and small regional variants in visible images.

Shadow can be classified into two types (Victor, et al., 2006): the self-shadow and cast-shadow. The former appears in self part of object where no light reaches. The latter appears in object surface which is cast by other object near to the illumination source. In this paper, we refer the shadow to the cloud cast-shadow. The shadow region is the area where the sun light is reflected by cloud and few spectral power sensed by sensor. In multi-spectral image, the shadows are of lower local intensity and small regional mean, and easily confused by water.

Two SPOT 4 multi-spectral images from the same area acquired in adjacent time are given in Fig. 1, the three bands are Green (0.50—0.59 μm), Red (0.61—0.68 μm) and NIR (0.78—0.89 μm) with spatial resolution of 20 m. The clouds are those bright white areas. Objects under thick clouds are completely not visible. Near the thick cloud edge, objects are partially visible. The shadow regions are those dark areas, and are often confused with water. As regard to the shape, clouds and shadows are irregular patches. The cloud and shadow keep a certain spatial relationship, with similar contours.

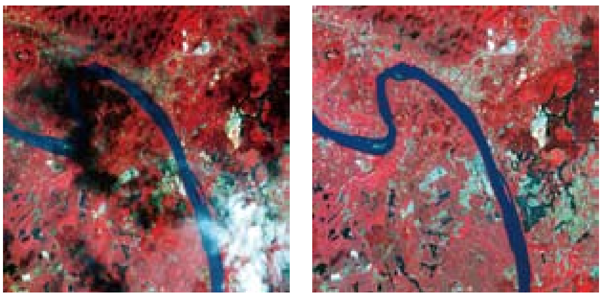

(a) The image to be repaired (b) The reference image

Fig. 1 Two SPOT 4 multi-spectral images from the same area acquired in adjacent time

3 DETECTION OF CLOUD AND SHADOW

According to the former analysis, there are great differences in the reflective intensity of shadow, cloud and other objects, the key to detection the cloud and shadow is to estimate a suitable threshold. Directly process in multi-spectral image is rather difficult. In order to extract cloud and shadow effectively, we perform fusion enhancement on cloud and shadow feature in YC_bC_r color space firstly to enlarge the contrast between cloud shadow and other object. The main procedures are as follows.

We note the three spectral channel data of image M as R, G, B. At first, M was transformed into YC_bC_r space using Eq. (1).

$$\begin{bmatrix} Y \\ C_b \\ C_r \end{bmatrix} = \begin{bmatrix} 0.257 & 0.504 & 0.098 \\ -0.148 & -0.291 & 0.439 \\ 0.439 & -0.368 & -0.071 \end{bmatrix} \begin{bmatrix} R \\ G \\ B \end{bmatrix} + \begin{bmatrix} 16 \\ 128 \\ 128 \end{bmatrix} \tag{1}$$

The shadow enhanced image and cloud enhanced one can be acquired with Eq. (2) and Eq. (3), respectively, where $f[\ ]$ represents the process of linear transform of the gray value into 0—255.

$$I_s = f[(C_b + C_r)/Y] \tag{2}$$

$$I_c = f[Y/I_s] \tag{3}$$

Fig. 2 shows the enhanced results of the image to be repaired in Fig. 1(a). It is obviously that after enhancement, the shadow and cloud are highlighted in their feature map respectively, and the contrasts with other object are also enlarged. Now, it is rather easy to find an appropriate segment threshold to detection the cloud and shadow. We use traditional Otsu's algorithm (Otsu, 1979) to find the optimal threshold T, which makes sure that

$$V(T) = \frac{[\mu \cdot w(T) - v(T)]^2}{w(T) \cdot v(T)} \tag{4}$$

where $w(T) = \sum_{i=0}^{T} p_i$, $v(T) = \sum_{i=T+1}^{255} p_i$, $\mu = \sum_{i=0}^{255} i \cdot p_i$, p_i represents the probability of pixel value equal to i.

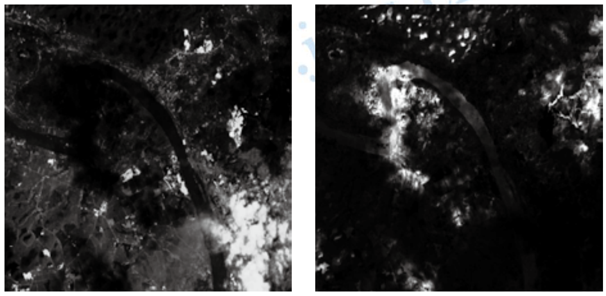

(a) Cloud enhancedresult (b) Shadow enhanced result

Fig. 2 The cloud and shadow enhanced results of the image to be repaired

Using Eq. (4) on shadow enhanced image I_s and cloud enhanced image I_c respectively, we can get the optimal threshold T_{sd}, T_{cd}. Then the preliminary shadow and cloud can be detected using the rule in Eq. (5) and Eq. (6).

$$M_{sd}(x,y) = \begin{cases} 1, & \text{if } I_s(x,y) \geqslant T_{sd} \\ 0, & \text{if } I_s(x,y) < T_{sd} \end{cases} \tag{5}$$

$$M_{cd}(x,y) = \begin{cases} 1, & \text{if } I_c(x,y) \geqslant T_{cd} \\ 0, & \text{if } I_c(x,y) < T_{cd} \end{cases} \tag{6}$$

Fig. 3 gives the detection result of cloud and shadow in image to be repaired. In preliminary results, it is inevitably that some highlight objects in multi-spectral image are false detected as cloud and some dark object as shadow. In order to improve the quality of repaired image, careful discriminations in post-processing are needed. Common method is to use morphological operation to discard isolated points, and then fill the segmented shadow and cloud regions, and compute the area, the ratio of length and width, etc, to further discriminate water from shadows, and buildings from clouds.

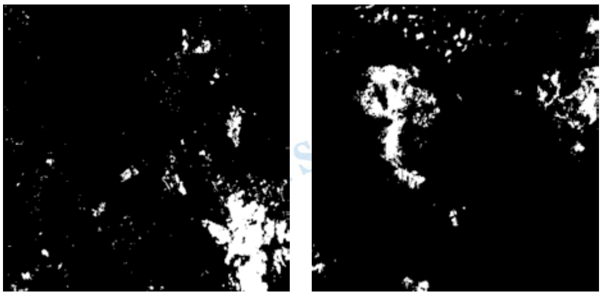

(a) Detected cloud regions (b) Detected shadow regions

Fig. 3 The detected cloud and shadow regions in image to be repaired

Considering that we have another image as reference, there will be of great intensity difference between the reference image and the image to be repaired in real cloud and shadow regions. Making full use of this feature, the discrimination in post-processing can be simplified greatly.

Assume that Y_1 and Y_2 are the intensity component of the image to be repaired and the reference one extracted using Eq. (1), then the potential shadow region M_{sp} and cloud region M_{cp} can be defined as

$$M_{sp}(x,y)=\begin{cases}1, & \text{if } Y_2(x,y)/Y_1(x,y)\geqslant T_{sp}\\ 0, & \text{if } Y_2(x,y)/Y_1(x,y)<T_{sp}\end{cases} \tag{7}$$

$$M_{cp}(x,y)=\begin{cases}1, & \text{if } Y_1(x,y)/Y_2(x,y)\geqslant T_{cp}\\ 0, & \text{if } Y_1(x,y)/Y_2(x,y)<T_{cp}\end{cases} \tag{8}$$

where T_{sp} and T_{cp} are intensity change threshold caused by shadow and cloud, respectively. Logic AND are performed on detected cloud and shadow region and the potential ones to get the final cloud and shadow detection result.

We then build the normalized cloud and shadow density map using Eq. (9) and Eq. (10), which reflects the concealed condition.

$$M_s=I_s M_{sd} M_{sp}/255 \tag{9}$$

$$M_c=I_c M_{cd} M_{cp}/255 \tag{10}$$

Fig. 4 gives the normalized cloud and shadow density map of the image to be repaired. It can be seen that the larger the density, the poorer the diaphaneity.

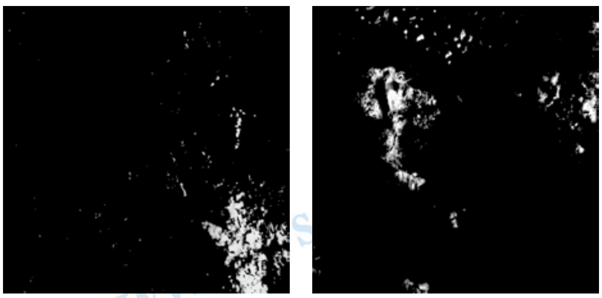

(a) Normalized cloud density map (b) Normalized shadow density map

Fig. 4 Normalized cloud and shadow density map of the image to be repaired

4 REPAIRING OF CLOUD AND SHADOW REGION

In order to get perfect repairing results and recover the concealed information as much as possible, different schemes are needed according to regions of different shadows or cloud densities. The main regulation is that regions of lower cloud and shadow density should make full use of the information from itself, while the regions of greater cloud and shadow density should mainly make use of the information from reference image. We design a two step scheme with linear combination followed by histogram matching to repair of cloud and shadow regions.

4.1 Linear combination

Linear combination is to repair the cloud or shadow regions by combination of the same from both images with linear weights in the direction of cloud and shadow density map. Suppose that I_{1n} and I_{2n} are the nth band from the image to be repaired and the reference ones, the result can be expressed as

$$I_n=(I_{2n}M_s+I_{1n}(1-M_s))(1-M_c)+I_{2n}M_c \tag{11}$$

According to the process of building the density map, $M_s{\cdot}M_c$=0, Eq. (11) can be further simplified as

$$I_n=I_{1n}+(I_{2n}-I_{1n})(M_s+M_c) \tag{12}$$

Using Eq. (12) to repair the data band by band, the concealed information can be well recovered. But the repaired regions may different in brightness from the adjacent regions. In order to overcome this shortcoming, we construct the cloud and shadow buffer regions, and use spectral histogram matching method to adjust the linear combined result to be consistent to its neighbor.

4.2 Construction of cloud and shadow buffer region

In order to improve cloud and shadow repairing results, we construct the buffer regions as the reference region for histogram matching, which is referred as cloud and shadow data buffer region. Fig. 5 gives the relationship of a typical shadow region M_{shad} and its buffer region M_{shad_buff}, and the cloud region M_{cloud} and its buffer region M_{cloud_buff}.

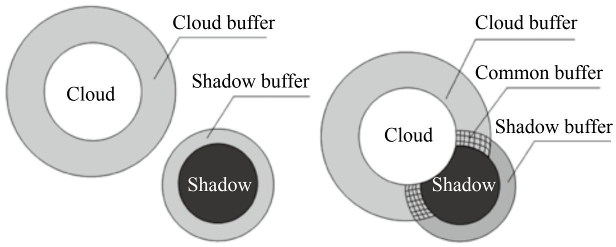

(a) Distance between cloud and shadow is large (b) Distance between cloud and shadow is small

Fig. 5 The relationship of cloud/shadow region and their buffer region

The method to construct different buffer regions on the basis of cloud and shadow detection result using morphological operation is as follows.

Suppose that m non-overlapped shadow regions M_{si} (i=1, 2, …, m) and n non-overlapped cloud regions M_{ci}(i=1, 2, …, n) were detected, the whole shadow regions can be defined as $M_{shad}=M_{s1}\cup M_{s2}\cup\ldots\cup M_{sm}$, and the whole cloud regions as $M_{cloud}=M_{c1}\cup M_{c2}\cup\ldots\cup M_{cn}$. Firstly, a circle structure $B(R_1)$ with radius R_1 was used to dilate the shadow regions, and the original shadow regions were subtract from the dilated result to get the shadow buffer regions

$$M_{si\_buff}=M_{si}\oplus B(R_1)-M_{si} \tag{13}$$

where ⊕ represents the morphological operation. Similarly, a circle structure $B(R_2)$ with radius R_2 was used to dilate the cloud region, and the original cloud regions were subtract from the dilated result to get the cloud buffer regions

$$M_{ci\_buff}=M_{ci}\oplus B(R_2)-M_{ci} \tag{14}$$

Considering that cloud and shadow may overlap, the influence between shadow buffer region and cloud buffer region must be discarded. The final cloud and shadow buffer region are as follows.

$$M_{si\_buff}=[M_{si}\oplus B(R_1)-M_{si}]\cap[1-M_{cloud}] \tag{15}$$

$$M_{ci\_buff}=[M_{ci}\oplus B(R_2)-M_{ci}]\cap[1-M_{shad}] \tag{16}$$

As shown in Fig. 5(b), when the distance of cloud and shadow is small, the constructed shadow buffer and cloud buffer may overlap to form a common buffer. The information from these common regions are useful for both shadow and cloud repairing.

4.3 Spectral histogram matching

Since the spectral characteristic in repaired regions should be of great similarity, we use spectral histogram matching to adjust the pixel values in preliminary repaired cloud and shadow regions into the expected value range in adjacent buffer regions, which will keep the repaired regions and their buffer regions consistent in brightness and tone. The principle is show in Fig. 6.

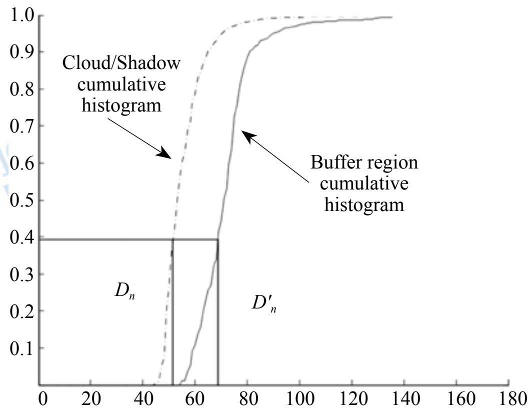

Fig. 6 The principle of spectral histogram matching

Suppose that D_n is the pixel value in cloud or shadow regions of n^{th} band in multi-spectral image which have been preliminary repaired. D'_n is the expected pixel value. The mapping relationship between then can be described as Eq. (17):

$$\sum_{i=1}^{D_n} p_{i,n}=\sum_{j=1}^{D'_n} q_{j,n} \tag{17}$$

where $p_{i,n}$ is the probability of the pixel value in cloud or shadow regions of n^{th} band to be i, $q_{j,n}$ is the probability of the pixel value in cloud or shadow regions of n^{th} band to be j. $\sum_{i=1}^{D_n} p_{i,n}$ and $\sum_{j=1}^{D'_n} q_{j,n}$ are corresponding cumulative histogram of cloud/shadow regions and their buffer regions.

Having constructed the pixel value mapping table between cloud/shadow regions and their corresponding buffer regions, the pixels in preliminary repaired regions can be further adjusted to obtain the final results. Fig. 7(a) gives the result of shadow regions been repaired.

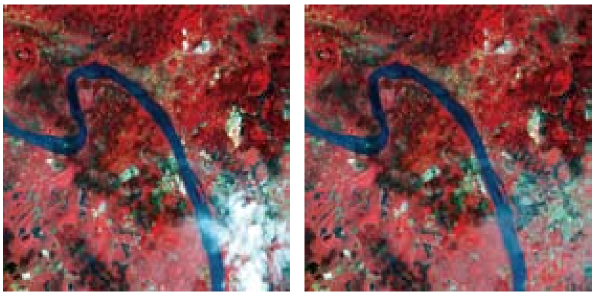

(a) Only the shadow region repaired (b) Both cloud and shadow repaired

Fig. 7 The repairing result of SPOT 4 image on Fig. 1(a)

5 EXPERIMENT RESULT AND ANALYSIS

The proposed algorithm is based on two images from the same area acquired in adjacent times. The thick clouds in both images should not overlap heavily, which is easy to be satisfied. In order to verify our algorithm, we choose two SPOT 4 multi-spectral

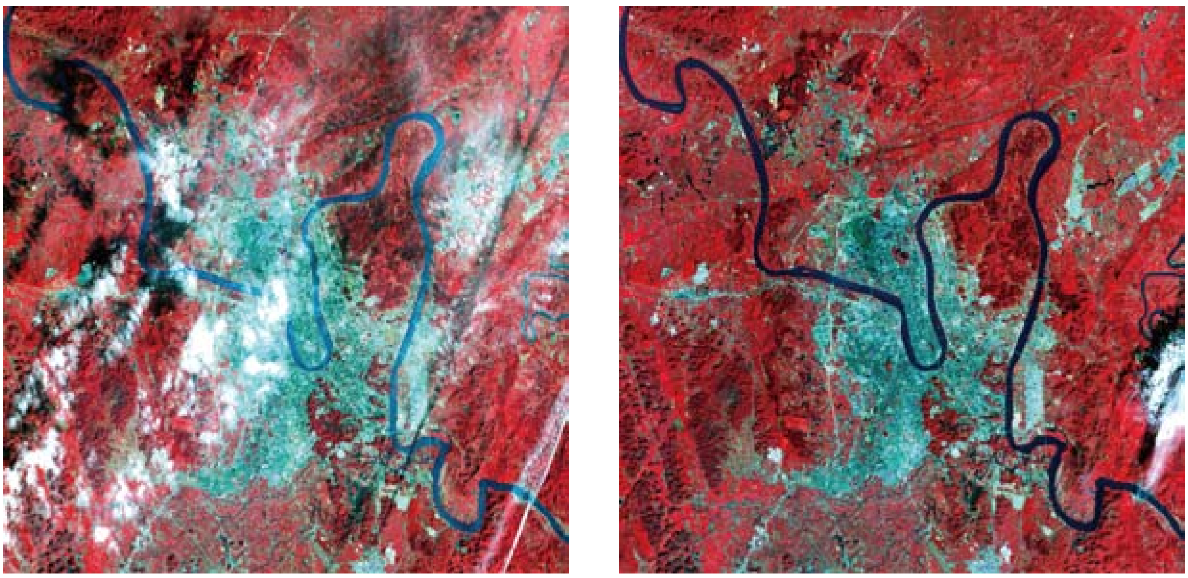

(a) Image to be repaired (acquired in 2010-10-05) (b) Reference image (acquired in 2010-10-06)

Fig. 8 Two SPOT 4 multi-spectral images acquired in adjacent time for experiment data covering the LIU Jiang drainage area near LIU Zhou City for validation. The spatial resolution is 20 m, three bands are Green (0.50—0.59 μm), Red (0.61—0.68 μm) and NIR (0.78—0.89 μm). The images are acquired in 2010-10-05 and 2010-10-06, respectively. Before experiment, we use ENVI to register the images, and adjust their brightness to be consistent. Then a local square region of 1664×1664 pixels was selected as the test area. As shown in Fig. 8, both of these two areas appear cloud and shadow, but their positions are not overlapped. We use the image which has much more cloud and shadow as the one to be repaired I_{main}, the other as the reference I_{ref}. Without any intervention, we get satisfied repairing effect.

During the process of cloud and shadow detection, we firstly fuse the multi-spectral image to enhance the cloud and shadow region respectively. Then we use Otsu's algorithm to find the optimal segmentation threshold to get preliminary cloud and shadow regions, in which T_{sp} and T_{cp} are set with 2 to get the potential regions. Logical AND operation is used to get the final cloud and shadow regions, and the normalized cloud and shadow density maps can then be constructed. We get the preliminary repairing result by linear combination of I_{main} and I_{ref} in the corresponding regions, and histogram matching algorithm were adopted to keep the consistent of repaired regions and their buffer regions. The final results are given in Fig. 9. It is obvious that the city and river partially concealed by cloud and shadow are well recovered, which greatly improves the visual effect and becomes more suitable for interpretation. We also note that there is a large patch of cloud and shadow on the right-down corner of the reference image. However, this did not influence the repair effect, because these regions are discarded automatically without any intervention.

The algorithm is implemented on Windows XP operation system with matlab 2008 on a PC with Pentium (R) D CPU 3.00 GHz, 2.00 GB physic memory. Many tests are carried out in SPOT 4 images. To repair the previous 1664×1664 image where nearly 30% pixels are cloud or shadow, the operations from reading the registered image to finish final repairing spent nearly 20 s in whole, which is very efficient.

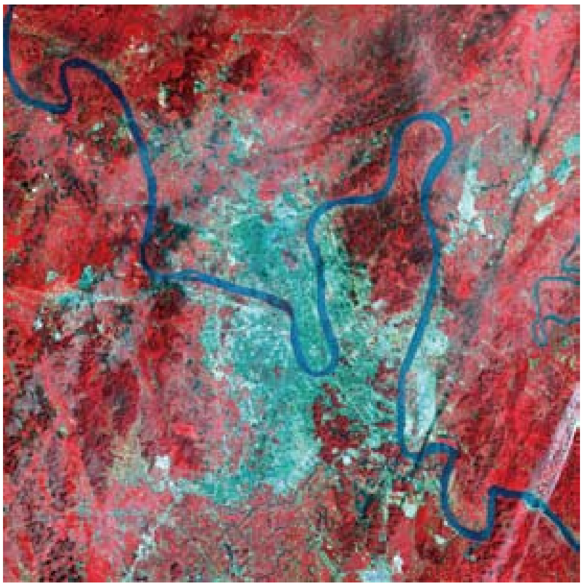

Fig. 9 The final repairing result on SPOT 4 image in Fig. 8(a)

For much larger images, it is reasonable to split them into several small patches, and then use the proposed algorithm to repairing. The detected cloud and shadow regions can also be used as the Mask region for other multi-source image replacement algorithm. In addition, by repairing the cloud and shadow band by band, our algorithm are also suitable for other data with more than three bands. The only change is to adjust the enhance method given in Eq. (1)—Eq. (3) according to the spectral feature of different sensors.

6 CONCLUSION

Elimination the influence of cloud and shadow to optical remote sensing image is a common problem during the process of image interpretation and applications. We proposed an effective algorithm for automatic detection and repairing of cloud and shadow regions in multi-spectral images. This algorithm make full use of both the spectral features of cloud and shadow and the local change caused by cloud or shadow between the image to be repaired and the reference one. Having constructed the normalized cloud and shadow density map, linear combination of two images and histogram matching algorithm were adopted to repair the shadow and cloud regions successively. The experiment on SPOT 4 multi-spectral image shows that clouds and shadows of different density can be well repaired, which can satisfied the need of many applications. In our future work, to increase the robustness and assess the repairing effect quantitatively should be further considered.

REFERENCES

Chai Y, He Y and Qu C W. 2010. Remote sensing image fusion using MGA based on cloud and shadow distance model. Journal of Image and Graphics, 15(9): 1398–1405

Otsu N. 1979. A threshold selection method from gray level histograms. IEEE Transactions on Systems Man and Cybernetics, 9(1): 62–69

RI Pyongsop, Ma Z B, Qi Q W and Liu G H. 2010. Cloud and shadow removal from Landsat TM data. Journal of Remote Sensing, 14(3): 534–545

Song X N and Zhao Y S. 2003. Cloud detection and analysis of MODIS image. Journal of Image and Graphics, 8(9): 1079–1083

Song X Y, Liu L Y, Li C J, Wang J H and Zhao C J. 2006. Cloud removing based on single remote sensing image. Optical Technique, 32(2): 299–303

Tsai V J D. 2006. A comparative study on shadow compensation of color aerial images in invariant color models. IEEE Transactions on Geoscience and Remote Sensing, 44(6): 1661–1671 DOI: 10.1109/TGRS.2006.869980

Wang S G, Li D R, Guo Z J and Zheng J L. 2004. Method for information processing of shadows and occlusion on orthophotos. Journal of Geomatics, 29(4): 1–4

Zhao Z M and Zhu Z G. 1996. Approach to removing cloud cover from satellite imagery. Environmental Remote Sensing, 11(3): 195–199

多光谱遥感影像中云影区域的检测与修复

周伟[1]，关键[1]，姜涛[2]，何友[1]

1. 海军航空工程学院 电子信息工程系，山东 烟台 264001
2. 海军航空工程学院 兵器科学与技术系，山东 烟台 264001

摘 要：提出了一种有效针对多光谱遥感影像的云影检测与阴影区域修复方法。基于同一地区时相相近的两幅影像，充分利用碎云及阴影的光谱特性分别对云影区域进行融合增强，然后采用Otsu算法求解最佳阈值自动检测出云及阴影区域，根据云影的出现会引起两幅影像局部相应区域明显的亮度变化，可排除亮地物和水体的影响，建立归一化的云影密度图，在此基础上，采用线性加权组合与光谱直方图匹配相结合的方法对其加以修复，利用SPOT 4影像进行的实验表明其修复效果完全能够满足应用需要。

关键词：自动检测，影像修复，直方图匹配，云影密度图，多光谱

中图分类号：TP751 **文献标志码**：A

引用格式：周伟，关键，姜涛，何友．2012．多光谱遥感影像中云影区域的检测与修复．遥感学报，16(1): 132–142
Zhou W, Guan J, Jiang T and He Y. 2012. Automatic detection and repairing of cloud and shadow regions in multi-spectral remote sensing images. Journal of Remote Sensing, 16(1): 132–142

1 引 言

光学卫星在成像过程中不可避免会受到云雾的影响，在获取的遥感影像上经常会出现块状的高亮区域及暗淡的阴影区域，使得对应区域所反映的被摄目标信息有所损失或受到干扰，从而直接影响目标检测、识别和地物分类的正确率，给遥感影像的判读解译和应用造成较大困难(王树根 等，2004)。如何检测并修复遥感影像受云及阴影的影响的区域(宋小宁和赵英时，2003；宋晓宇 等，2006；柴勇 等，2010)，是许多应用者所面临的首要问题。

云影处理算法会随云的覆盖类型的不同而不同，稀薄的云雾会使得影像模糊，但是地物未被完全遮挡，为有效去除大范围内存在的薄云，赵忠明和朱重光(1996)提出了同态滤波去云法，把频率过滤与灰度变化结合起来，分离云与背景地物，最终从影像中消除云的影响，这种方法由于涉及滤波器结构以及截止频率的选择，在滤波的过程中有时会丢失一些有用信息。大面积的厚云，不仅遮蔽传感器视线方向的部分地物，而且会在地面投射出大块的阴影，目前比较有效的方法是同相近时相或不同年份同一季节的无云数据对厚云区域进行替换修复(李炳燮 等，2010)，但是受地物和成像条件变化的影响，其修复效果取决于无云数据与待修复数据的相似程度，而且需要对多源数据进行精确的配准和校正，处理周期比较长。

在沿海地区，晴好天气也经常会有若干大小不等的碎云漂浮在中低空，尽管获取的光学遥感影像整体视觉效果良好，但是影像中局部出现的形态各异的云及其阴影会遮蔽部分地物，从而给影像的判读解译及情报产品制作带来困难。本文提出了一种有效的针对多光谱影像的云影自动检测与修复方法，该方法基于同一地区时相相近的两幅影像，充分利用云及阴影的光谱特性分别对云及阴影区域进行融合增强，然后采用Otsu (1979)算法求解最佳阈值自动检测出云影区

收稿日期：2010-10-22；**修订日期**: 2011-06-21
基金项目：国家自然科学基金（编号: 60672140，60802088）；航空科学基金（编号: 20095184004）
第一作者简介：周伟(1980—)，男，讲师，博士研究生。研究方向为侦察图像处理、目标检测与识别。E-mail: yeaweam@gmail.com。
通信作者简介：关键(1968—)，男，教授，博士生导师。研究方向为雷达目标自动检测、侦察图像处理和信息融合。E-mail: guanjian96@tsinghua.org.cn。

域，利用云影会导致两幅影像局部相应区域出现明显亮度差异的特点排除高亮地物和水体的影响，建立归一化的云影密度图，根据云影区域的特点，采用线性加权组合与光谱直方图匹配相结合的方法对其加以修复。利用SPOT 4多光谱影像进行的实验，得到了较好的云影修复效果。

2 云及阴影的特性分析

从遥感物理的角度，云属于大气气溶胶的范畴，是地球大气中具有一定稳定性，沉降速度小，尺度范围在10^{-3}—10 μm之间的液态离子或固态离子所组成的混合物集合体。从云层的反射特性来看，在可见光波段云层属于漫反射物体，体现在可见光遥感影像中，含云区域具有局部能量大，区域灰度均值高、方差小的特点。

阴影可以分为两类(Tsai，2006)：一是由遮挡物体自身没有被光源照射到而产生的，称为本影(Self-Shadow)；一是由一物体遮挡住光源从而在另一物体表面产生的阴影，称为投影(Cast-Shadow)。本文讨论的阴影是云的投影，即由于入射的光线被云层遮挡导致反射进入遥感传感器的光谱能量较小而形成的，在多光谱遥感影像上表现为局部能量较小，区域灰度均值较低的特点，容易与水体相混淆。

图1给出同一区域时相相近的二幅SPOT 4多光谱影像(3个波段分别为绿：0.50—0.59 μm，红：0.61—0.68 μm和近红：0.78—0.89 μm，分辨率为20 m)。浮云在多光谱影像中表现为接近白色的区域，云层较厚处的地物完全不可见，接近边缘处逐渐稀薄，地物部分可见。而阴影区域表现为较暗的区域，视觉上容易与水体相混淆。在几何外形上云影多为团块状且极不规则，在空间关系上云影通常同时出现且保持特定的位置关系，外形轮廓也有一定的相似性。

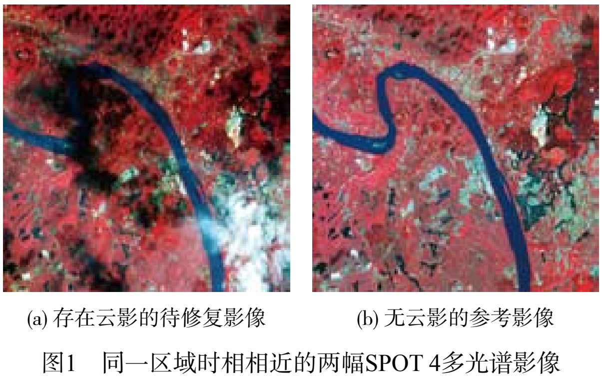

(a) 存在云影的待修复影像　(b) 无云影的参考影像

图1 同一区域时相相近的两幅SPOT 4多光谱影像

3 云及阴影的检测

通过前面的分析可以看出，碎云和阴影与其他地物在反射强度上存在较大差异，分别估计合适阈值即可检测出云和阴影区域。直接在多光谱图像上操作是很困难的，为了确保云和阴影的提取效果，我们首先在YC_bC_r空间对云影特征进行融合增强处理，进一步加大云影与其他地物间的反差，具体方法如下：

记待修复多光谱影像M的三通道数据分别为R、G和B，首先将M变换到YC_bC_r空间，

$$\begin{bmatrix} Y \\ C_b \\ C_r \end{bmatrix} = \begin{bmatrix} 0.257 & 0.504 & 0.098 \\ -0.148 & -0.291 & 0.439 \\ 0.439 & -0.368 & -0.071 \end{bmatrix} \begin{bmatrix} R \\ G \\ B \end{bmatrix} + \begin{bmatrix} 16 \\ 128 \\ 128 \end{bmatrix} \tag{1}$$

阴影特征增强影像为：

$$I_s = f[(C_b + C_r)/Y] \tag{2}$$

碎云特征增强影像为：

$$I_c = f[Y/I_s] \tag{3}$$

式中，$f[\,]$表示影像灰度值线性拉伸至0—255的操作。

图2给出了利用上述方法分别对图1中的待修复影像进行云影增强的结果，可以看出，经融合增强处理以后，碎云和阴影区域均对应于高亮部分，且与其他地物形成较大的反差。这样一来，我们很容易分别在碎云和阴影特征增强影像上寻求合适的分割阈值来完成碎云及阴影的检测。本文中，我们利用经典的Otsu (1979)方法来寻找最优阈值T，使得：

$$V(T) = \frac{[\mu \cdot w(T) - v(T)]^2}{w(T) \cdot v(T)} \tag{4}$$

式中，$w(T) = \sum_{i=0}^{T} p_i$，$v(T) = \sum_{i=T+1}^{255} p_i$，$\mu = \sum_{i=0}^{255} i \cdot p_i$，$p_i$表示影像中灰度值为$i$个概率。

利用上述方法得到阴影增强影像I_s和云增强影像I_c的最优阈值T_{sd}，T_{cd}后，根据式(5)、(6)两个判决式

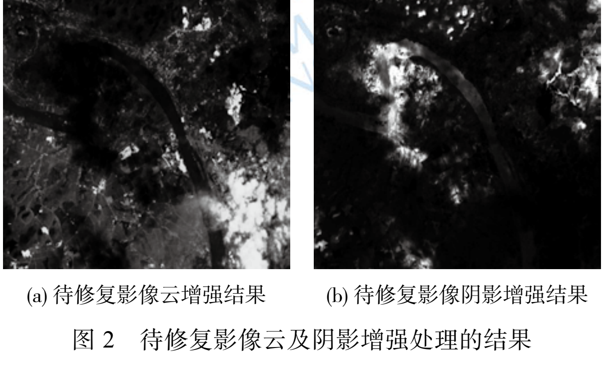

(a) 待修复影像云增强结果　(b) 待修复影像阴影增强结果

图 2 待修复影像云及阴影增强处理的结果

就可以分别得到阴影和云的初步检测结果。

$$M_{sd}(x,y)=\begin{cases}1, & \text{if } I_s(x,y)\geqslant T_{sd}\\ 0, & \text{if } I_s(x,y)<T_{sd}\end{cases} \tag{5}$$

$$M_{cd}(x,y)=\begin{cases}1, & \text{if } I_c(x,y)\geqslant T_{cd}\\ 0, & \text{if } I_c(x,y)<T_{cd}\end{cases} \tag{6}$$

图3给出了利用上述方法得到的图1中待修复影像的云及阴影检测结果，在检测出的云和阴影区域，不可避免会有部分高亮地物被误判为云，部分低亮度的地物被误判为阴影，为了提高云影修复质量，通常需要在后处理阶段加以鉴别。常规的处理方法是利用形态学运算对孤立的目标点加以剔除，并将各个碎云和阴影区域填充完整，再利用区域的面积、长宽比等形状特征对阴影和水体、云和高亮的建筑等加以区分。

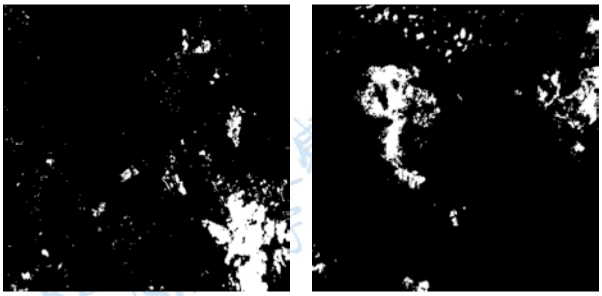

(a) 待修复影像碎云检测结果　(b) 待修复影像阴影检测结果

图3　待修复影像云及阴影检测的结果

考虑到进行修复时还有一幅参考影像，则在出现云影的区域，参考影像和待修复影像将表现出明显的亮度差异。充分利用这一特点，则云影检测结果的鉴别过程可以大大简化。

设Y_1和Y_2分别为利用式(1)得到的待修复影像和参考影像的亮度分量，潜在阴影区域M_{sp}和潜在云区域M_{cp}可分别用下式求得：

$$M_{sp}(x,y)=\begin{cases}1, & \text{if } Y_2(x,y)/Y_1(x,y)\geqslant T_{sp}\\ 0, & \text{if } Y_2(x,y)/Y_1(x,y)<T_{sp}\end{cases} \tag{7}$$

$$M_{cp}(x,y)=\begin{cases}1, & \text{if } Y_1(x,y)/Y_2(x,y)\geqslant T_{cp}\\ 0, & \text{if } Y_1(x,y)/Y_2(x,y)<T_{cp}\end{cases} \tag{8}$$

式中，T_{sp}、T_{cp}分别为阴影和云所引起的影像亮度变化阈值，将云影检测的结果与云影潜在区域进行与运算，即得到最终的云影检测结果。

在此基础上，我们可以进一步用式(9)和式(10)构建阴影和云的归一化密度图，用以直观地反映云影对地物的遮蔽程度。

$$M_s=I_s M_{sd} M_{sp}/255 \tag{9}$$

$$M_c=I_c M_{cd} M_{cp}/255 \tag{10}$$

图4给出了待修复影像的归一化云和阴影的密度图，显然密度越大，透视性越差。

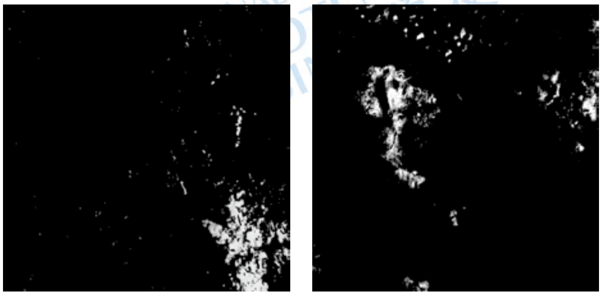

(a) 归一化云密度图　(b) 归一化阴影密度图

图4　待修复影像归一化云影密度图

4　云及阴影的修复

为了取得好的修复效果，尽可能还原被遮蔽的信息，针对不同密度的云影区域应采取不同的修复方法。需要遵循的原则是，对于密度较小的云影区域，应充分利用待修复影像自身的信息，而对于密度较大的云影区域，则主要利用参考影像的信息，为此我们设计了线性加权组合与光谱直方图匹配相结合的方法进行云影区域的修复。

4.1　线性加权组合

线性加权组合就是在云影密度图的指导下，将待修复影像和参考影像对应区域线性加权组合的方式加以修复。设I_{1n}和I_{2n}分别表示待修复影像和参考影像的第n个波段的数据，则云影修复结果I_n可表示为：

$$I_n=(I_{2n}M_s+I_{1n}(1-M_s))(1-M_c)+I_{2n}M_c \tag{11}$$

由云影密度图的求解过程可知，$M_s \cdot M_c=0$，则上式可进一步简化为：

$$I_n=I_{1n}+(I_{2n}-I_{1n})(M_s+M_c) \tag{12}$$

利用式(10)对各个通道的数据逐一加以修复，可较好地恢复不同密度的云影所遮蔽的信息，但是修复区域可能会与其临近区域在整体亮度上有所差别。为了克服这一问题，可分别构建云影的缓冲区，然后采取光谱直方图匹配的方法来调整经初步修复的云影区像素值，使其亮度和色调与缓冲区一致。

4.2　云影缓冲区的构建

为了进一步改善云影修复效果，将临近云影的局部区域构建作为光谱匹配的参考区，称为云影数

据缓冲区。图 5给出了典型的阴影区域M_{shad}及其缓冲区M_{shad_buff}和云区域M_{cloud}及其缓冲区M_{cloud_buff}的相互关系。下面给出借助形态学方法在云影检测结果的基础上分别构建各个云影区域的缓冲区的具体方法。

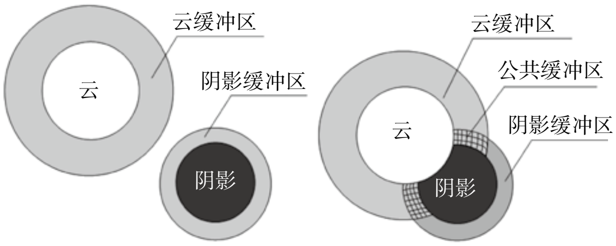

(a) 云影间距离较大的情形 (b) 云影间距离较小的情形

图5 碎云、阴影区域及相应缓冲区示意图

设分别检测到m块互不交叠的阴影$M_{si}(i=1, 2, \cdots, m)$和$n$块互不交叠的碎云$M_{ci}(i=1, 2, \cdots, n)$，则全部阴影区域$M_{shad}=M_{s1}\cup M_{s2}\cup\cdots\cup M_{sm}$，全部碎云区域$M_{cloud}=M_{c1}\cup M_{c2}\cup\cdots\cup M_{cn}$，首先用半径为$R_1$的圆形结构元素$B(R_1)$对阴影区域$M_{si}$进行膨胀运算，再从结果中减去阴影区域即得到相应的缓冲区：

$$M_{si\_buff}=M_{si}\oplus B(R_1)-M_{si} \tag{13}$$

式中，$\oplus$表示形态学膨胀运算。同理，用半径为R_2的圆形结构元素$B(R_2)$对碎云区域M_{ci}进行膨胀运算，再从结果中减去碎云区域即得到相应的缓冲区：

$$M_{ci\_buff}=M_{ci}\oplus B(R_2)-M_{ci} \tag{14}$$

考虑到云影可能交叠的情况，需要从阴影缓冲区中排除云的影响，同时云缓冲区也要排除阴影的影响，则最终的云影缓冲区分别表示为：

$$M_{si\_buff}=[M_{si}\oplus B(R_1)-M_{si}]\cap[1-M_{cloud}] \tag{15}$$

$$M_{ci\_buff}=[M_{ci}\oplus B(R_2)-M_{ci}]\cap[1-M_{shad}] \tag{16}$$

在云影距离较小的情况下，利用上述方法建立的云缓冲区和阴影缓冲区可能有部分交叠，即出现类似图5(b)中的公共缓冲区，该区域的信息对于云和阴影的修复都具有参考价值。

4.3 光谱直方图匹配

考虑到云影区域地物光谱特性与其临近区域地物具有很强相似性的特点，我们直接采用光谱直方图匹配方法，将初步修复的云影区域所对应的多个光谱波段数据的辐射值分别调整到其临近区域相应的数据范围，也就是使其在亮度和色调上与缓冲区保持一致。其原理如图 6所示。

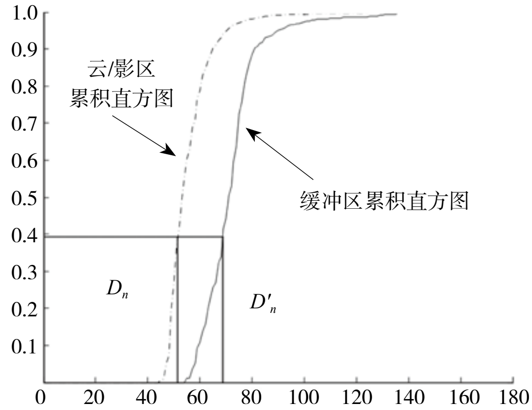

图6 光谱直方图匹配原理示意图

记D_n为多光谱影像第n个波段处于云影区的像素灰度值，D'_n为期望的灰度值，两者之间的映射关系可以通过求解式(17)得到：

$$\sum_{i=1}^{D_n} p_{i,n}=\sum_{j=1}^{D'_n} q_{j,n} \tag{17}$$

式中，$p_{i,n}$为多光谱影像第n个波段云影区像素灰度值为i的概率，$q_{j,n}$为多光谱影像第n个波段云影缓冲区像素灰度值为j的概率，$\sum_{i=1}^{D_n} p_{i,n}$和$\sum_{j=1}^{D'_n} q_{j,n}$分别对应于图5中云影区和缓冲区的累积直方图。

分别求得云影区不同光谱波段的灰度映射表后，再据此将经初步修复的各个光谱波段云影区域的像素逐一修正，即完成了云影的修复。图7(a)、(b)分别给出了先后消除图1所示SPOT 4影像中的阴影和云区所得到的结果。

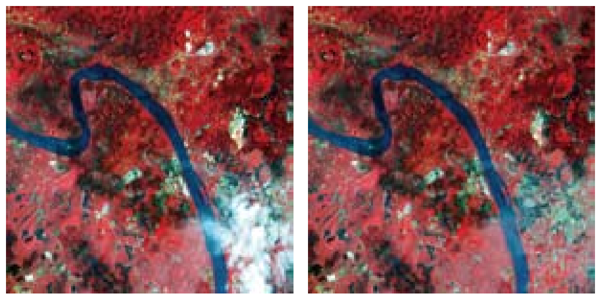

(a) 图1阴影修复结果 (b) 图1云区修复结果

图7 SPOT 4多光谱影像云影区域修复结果

5 实验结果与分析

本文方法基于同一地区时相相近的两幅影像，要求待修复影像和参考影像中厚云出现的位置不重叠，这在实际工作中是非常易于满足的。为了对本文算法加以验证，我们选取覆盖柳江流域柳州段的两幅

SPOT 4多光谱数据进行实验，数据分辨率为20 m，3个波段分别为绿波段、红波段和近红外波段，成像时间分别为2010-10-05和2010-10-06，借助ENVI或PCI等遥感处理软件，对两幅影像进行高精度的配准和整体亮度校正后，分别选取大小为1664×1664试验区域(图8)。两幅影像均存在不同程度的云及阴影，但出现位置几乎不交叠。将云影较多的作为待修复影像I_{main}，受云影影响较小的作为参考影像I_{ref}，在无需人工干预的情况下，获得了较为满意的修复效果。

在碎云和阴影的检测过程中，首先对云和阴影进行融合增强，然后采用Otsu方法寻找云影的最优分割阈值，得到初步云影检测结果，将T_{sp}和T_{cp}均设置为2，得到云影的潜在区域，然后分别进行与运算，即得到最终的云影检测结果，构建归一化云影密度图，在此基础上，采用线性加权组合与光谱直方图匹配相结合的方法对其加以修复，最终的修复结果如图9所示。可以看见，局部受云及阴影遮蔽的城区和河流均得到了有效的修复，极大地改善了影像的视觉效果，更易于判读解译。我们还注意到在参考影像的右侧存在大块的云影，但是这并不会对影像的修复产生干扰。应用本文的云影检测方法，这些区域可以被自动排除，无需人工干预。

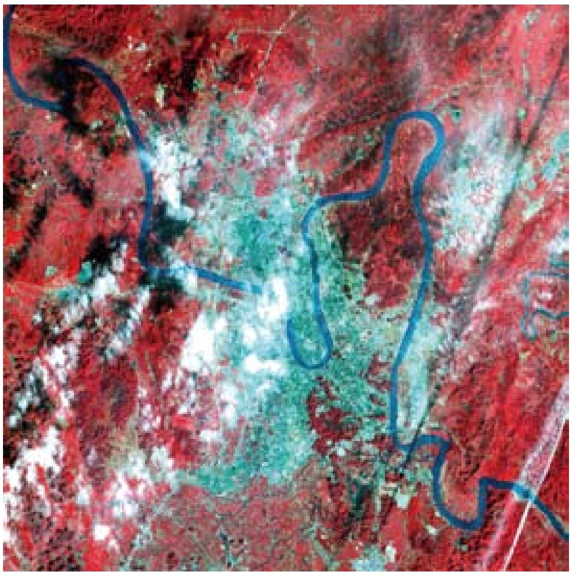

(a) 待修复影像(成像时间为2010–10–05)

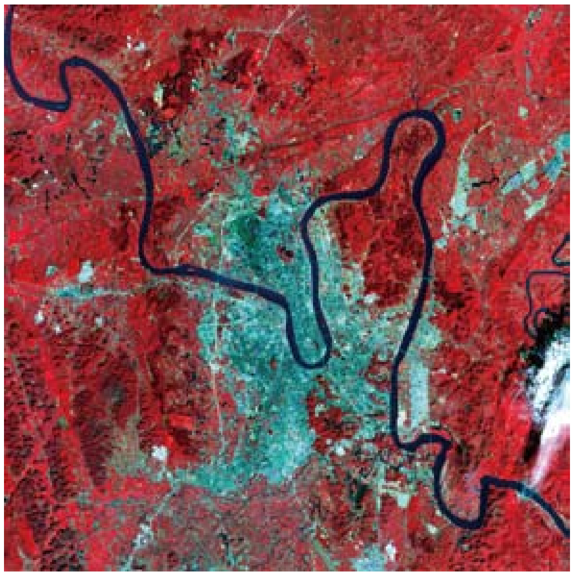

(b) 参考影像(成像时间为2010–10–06)

图8　本文实验用到的两幅时相相近的SPOT 4影像

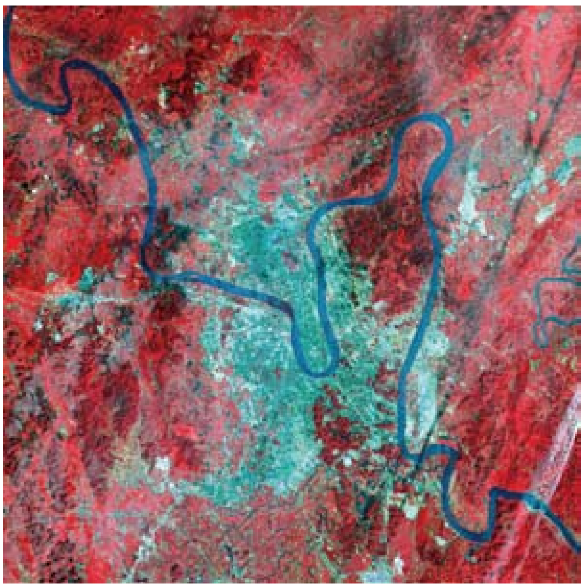

图9　SPOT 4多光谱影像云影区域修复结果

在Windows XP系统下用matlab2008编程实现上述算法，在Pentium(R) D CPU 3.00 GHz, 2.00 GB内存的PC机上对多组SPOT 4影像进行云及阴影的检测与修复实验。对大小为1664×1664，云影量约30%的实验影像，从读入经配准的数据到完成最终修复，总运行时间约为20 s左右，处理速度很快。

而对于更大面积的影像，可以考虑首先将其划分为若干小块，然后逐块采用本文算法加以修复。利用本文算法快速检测出的云和阴影区域也可以作为其他修复算法的多源数据替换区域掩模，另外，由于本文对云和阴影的修复是逐光谱通道进行的，因此对于更多通道的多光谱数据，本文的基本流程仍然适用，仅需根据不同遥感数据的特点对式(1)—(3)给出的云影融合增强方法作适当调整。

6 结 论

消除光学遥感影像受云及阴影的影响是遥感影像判读解译和应用过程中经常遇到的问题，本文提出了一种有效的针对多光谱遥感影像的云影检测与阴影区域修复方法。该方法充分利用了云及阴影的光谱特性及其在两幅相近时相影像上引起的局部差异，构造归一化云影密度图，采取多时相线性加权组合与光谱直方图匹配相结合的方法进行云影的快速修复。利用SPOT 4多光谱数据进行的实验表明不同密度的云影均可得到较好的修复，完全能够满足应用需要。后续我们将围绕提高算法的稳健性和定量评价修复效果等作进一步的研究。

参考文献(References)

柴勇, 何友, 曲长文. 2010. 基于云影距离模型的遥感图像多尺度融合算法. 中国图象图形学报, 15(9): 1398-1405

Otsu N. 1979. A threshold selection method from gray level histograms. IEEE Transactions on Systems Man and Cybernetics, 9(1): 62-69

李炳燮, 马张宝, 齐清文, 刘高焕. 2010. Landsat TM 遥感影像中厚云和阴影去除. 遥感学报, 14(3): 534-545

宋小宁, 赵英时. 2003. MODIS图象的云检测及分析.中国图象图形学报, 8(9): 1079-1083

宋晓宇, 刘良云, 李存军, 王纪华, 赵春江. 2006. 基于单景遥感影像的去云处理研究. 光学技术, 32(2): 299-303

Tsai V J D. 2006. A comparative study on shadow compensation of color aerial images in invariant color models. IEEE Transactions on Geoscience and Remote Sensing, 44(6): 1661-1671 DOI: 10.1109/TGRS.2006.869980

王树根, 李德仁, 郭泽金, 郑精灵. 2004. 正射影像上阴影和遮蔽的信息处理方法研究. 测绘信息与工程, 29(4): 1-4

赵忠明, 朱重光. 1996. 遥感图象中薄云的去除方法. 环境遥感, 11(3): 195-199